scientific reports

Check for updates

OPEN

Automated system for establishing standard radiation dose–response curves and dose estimation for the Korean population

Su Jung Oh[1,4], Min Ho Jeong[2,4], Yeong-Rok Kang[1], Chang Geun Lee[1], HyoJin Kim[1], Yong Uk Kye[2], Moon-Taek Park[1], Jeong-Hwa Baek[1], Jung-Ki Kim[1], Joong Sun Kim[3], Soo Kyung Jeong[1]✉ & Wol Soon Jo[1]✉

Biological dosimetry is crucial for estimating the doses from biological samples and guiding medical interventions for accidental radiation exposure. This study aimed to derive rapid and precise dose estimates using a dicentric chromosome assay. To address the challenges of manual scoring of dicentric chromosomes, we upgraded an automatic system aimed at enhancing the precision of dicentric chromosome detection while reducing the need for human intervention. We collected blood from 30 individuals aged 20–67 years to create 30 dose-response curves aiming to investigate the differences in responses among individuals. To validate dose-estimate accuracy within a 95% confidence interval, blinded samples were categorized into three groups according to the radiation dose as follows: ≥2, ≤1, and 0.1 Gy. When scoring dicentric chromosomes without human review and constructing a dose–response curve, individual differences were observed. For doses ≤1 Gy, the standard root formula was effective; conversely, for doses ≥2 Gy, the regression deep neural network proved to be more ac-curate. Our developed program allowed for the rapid analysis of a large volume of dicentric chromosome images.

The safe use and management of radiation are becoming increasingly critical. As the application of radiation has expanded across various sectors, including healthcare, industry, military, and scientific research, the awareness of associated risks has increased[1,2]. Additionally, the expansion of aerospace exploration has brought the exposure to cosmic radiation to the forefront as a new area of concern[3–5]. Therefore, an increasing need exists for radiation-exposure assessments not only to respond to radiation accidents and terrorism threats but also to monitor occupational radiation exposure. In particular, exposure levels > 1 Gy can lead to acute radiation syndrome (ARS), whereas those < 1 Gy necessitate long-term monitoring because of the risk of late stochastic effects such as cancer[6–9].

Biodosimetry is the process of estimating radiation dose based on changes in biological markers post-exposure, and the dicentric chromosome assay (DCA) is considered the "golden standard" owing to its radiation specificity and low background levels of dicentric chromosomes[10]. However, manual DCA is time-consuming and requires expert human analysis, making it challenging to process large numbers of samples, such as in the event of a major radiological disaster or for health monitoring of occupational radiation exposure[10,11]. To overcome this limitation, research has been conducted to evaluate large sample volumes in the triage mode[12–14], and interlaboratory comparison studies for coordinated response[15–18] have been actively pursued.

Automated systems that can swiftly detect dicentric chromosomes have recently been introduced, facilitating ongoing research[19–22]. However, these systems have not entirely replaced humans. To bridge this gap, a solution has been adopted where automated assessments are subject to human review, thereby enabling the expedited determination of exposure levels[23–25]. Notably, these systems facilitated the successful construction of dose–response curves from the blood donations of 10 individuals[25].

In a previous study, we successfully established dose–response curves for dicentric chromosomes using an automatic system without human intervention[26]. In this study, we extended our work by utilizing an upgraded

[1]Dongnam Institute of Radiological and Medical Sciences (DIRAMS), 40 Jwadong-gil, Jangan-eup, Gijang-gun, Busan 46033, Republic of Korea. [2]Department of Microbiology, Dong-A University College of Medicine, Daeshingongwon-gil 32, Seo-gu, Busan 49236, Republic of Korea. [3]College of Veterinary Medicine and BK21 Plus Project Team, Chonnam National University, 77 Yongbong-ro, Buk-gu, Gwangju 61186, Republic of Korea. [4]Su Jung Oh and Min Ho Jeong contributed equally to this work. ✉email: soo87@dirams.re.kr; sailorjo@dirams.re.kr

automatic system[27] aiming to investigate potential variations in dose–response curves among individuals. Furthermore, building upon this foundation, we examined techniques for obtaining reliably estimated doses by creating various blinded samples with doses ranging from 0.1 to 4 Gy.

Results

Analyzing variabilities in dose–response curves

To construct dose–response curves, blood samples were collected from 30 Korean volunteers, comprising 14 females and 16 males, ranging in age from the early 20s to 60s. We then exposed these samples to radiation and analyzed the dicentric chromosome frequency to observe individual differences in the dose–response curve. To construct the dose–response curves of the 30 participants, we utilized the biodosetool package in R[28]. This approach enabled us to fit 30 dose–response curves with 95% confidence intervals for the upper and lower curves. However, specific data points, namely 0.5 and 3 Gy from dose–response curves 12 and 21, respectively, adversely influenced the fitting process. Therefore, these points were excluded from the fitting to ensure the accuracy and reliability of the curve estimation.

Initially, we determined whether the dose–response curves were differently fitted according to age and sex. To determine whether any differences were associated with sex, we fitted the curves separately for each sex. When 30 standard curves color-coded by sex were visualized, the curves appeared to be dispersed rather than clustered (Fig. 1a). To statistically verify whether any sex-linked differences exist, we pooled data by sex and fitted a dose–response curve for each (Table 1; Fig. 1b). Subsequent z-test analysis[29] confirmed that no significant difference exists in the curves between both sexes (α coefficient p-value = 0.39; β coefficient p-value = 0.65).

Next, we investigated whether a correlation exists between the 30 dose–response curves and age. Because the ages were obtained under diverse conditions, rather than comparing the entire curves, we focused our analysis on the 4 Gy point, where the differences were most pronounced. The results yielded a correlation coefficient (r) of -0.56, indicating an unclear correlation. Because of this ambiguity, we further explored the data using hierarchical clustering.

In this analysis, rather than relying on the directly observed frequency of dicentric chromosomes after 4 Gy of exposure, we employed the predicted y-values derived from the dose–response curve at 4 Gy. The dendrogram illustrates the grouping of the data points. We categorized the samples into six groups (cluster height = 0.1), applied color codes to the dose–response curves, and compared them with the age of each sample (Fig. 1c). As shown in Fig. 1d; Table 2, the age of the participants appeared to influence the slopes of the curves to some extent. Specifically, the first three groups, A, B, and C, with mean ages of 20, 27.4, and 36.8 years, respectively, showed a decreasing slope with age. Conversely, the subsequent groups, D, E, and F, presented with mean ages in the 40s, with no significant alteration in age difference compared to the preceding three groups. Group D encompassed the broadest age range, which included participants in their late 20s to those in their late 60s. This analysis suggests that while individual dose–response curves exhibit variability and a tendency based on age, relying on age information to select a dose–response curve for estimating the dose of a blinded sample using an automatic system could be precarious because of inherent risks.

Estimating dose for blinded samples for ≥ 2 Gy

Rapid and accurate dose assessments of radiation accident victims are crucial. In particular, doses exceeding 1 Gy can lead to ARS, which requires accurate dose assessment for appropriate medical response and treatment planning[6,30,31]. To verify the reliability of the dose assessments for doses > 1 Gy, we tested blinded samples using the automated system. Blinded samples were obtained from the blood of three healthy adults, different from those used to construct the dose–response curve, and were exposed to radiation doses of 2, 3, and 4 Gy. The samples were subjected to the same processing procedure used to construct the dose curves.

We first calculated the estimated doses using a pooled dose–response curve from 30 individuals (Table 3, Fig. 2a, and Supplementary Table S1). A sample was marked "valid" if the actual dose was within the 95% confidence interval of the estimated dose; otherwise, it was considered "invalid." Of the nine samples, five were fitted, but four were overestimated compared to the actual doses.

For participant B1, a 30-year-old female, all doses (2, 3, and 4 Gy) were valid when assessed against the pooled dose–response curve based on the frequency of identified dicentric chromosomes. However, for B2, a 36-year-old male, all doses were overestimated. For B3, a 34-year-old male, the samples irradiated with 2–3 Gy were valid; however, the sample irradiated with 4 Gy was overestimated. To determine whether these discrepancies arose from the dose–response curve, we recalculated the estimated doses for the nine blinded samples by dividing the dose–response curve into six groups (Table 4; Fig. 2b, and Supplementary Table S2). Group C showed the most favorable outcomes, with seven out of nine samples deemed valid according to the associated dose–response curve. Furthermore, we calculated the estimated doses for the 9 blinded samples using 30 individual dose–response curves, resulting in 106 of 270 possible outcomes (30 dose–response curves × 3 donors × 3 doses) (Fig. 2c). Among these, 25 of the 90 outcomes (30 dose–response curves × 3 donors) were consistent across all three doses for each of the three blood samples.

The applicable dose–response curve was obtained from 13 individuals, mostly in their 30s, including three in their 20s, one in their 40s, one in their 50s, and one in their 60s. Additionally, the dose–response curve that resulted in all three doses being valid for the three donors was generated from curves 3, 12, and 19, created using blood from 32-, 23-, and 34-year-old females, respectively.

These results highlight the importance of selecting appropriate dose–response curves to calculate the estimated doses when using an automatic system. However, the selection of a dose–response curve remains challenging. When estimating doses using blood from individuals exposed to radiation and analyzing dicentric chromosomes, the most readily available information about the samples is sex or age. While some correlation appears to exist with age, instances occurred where using a dose–response curve from a similar age group did

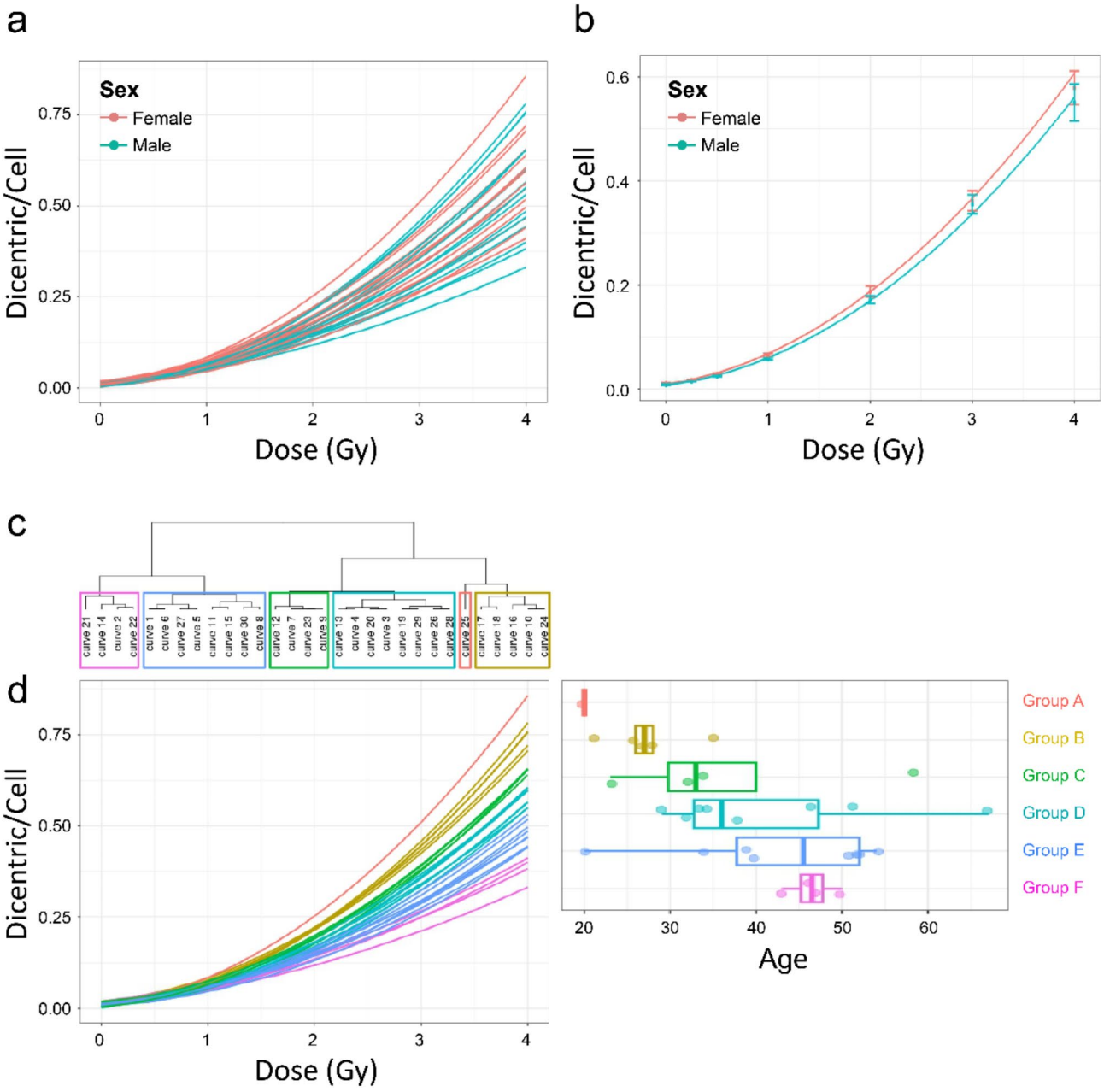

Fig. 1. The effect of sex and age on the dose-response curves of dicentric chromosome aberrations in 30 Korean volunteers. (**a**) Effect of sex on the dose–response curves of a dicentric chromosome. (**b**) Two dose–response curves pooled by sex. Error bars represent standard errors of the dicentric yield calculated from data obtained from 14 female and 16 male participants. (**c**) Dendrogram depicting data clustering based on the dicentric chromosome yield at 4 Gy, with clusters outlined in a box using a height threshold of 0.1. (**d**) Color-coded representation of the dose–response curves based on clustered groups. The right side of the box plot shows the age distribution in each group.

not result in valid estimations. In the case of curve 30, blood donated by a 34-year-old male was used to create a dose–response curve. However, a blinded test of the B2 sample, derived from a similar age, yielded "invalid" results across all doses. Conversely, the blood from curve 26, which was donated by a 67-year-old male, provided fitting estimates for all doses for the blinded sample from the 30-year-old participant (B1). This discrepancy may be because individual differences in the frequency of dicentric chromosomes become more pronounced at higher radiation doses.

Estimating dose using RDNN artificial intelligence system

According to the IAEA guidelines, to estimate the dose for blinded samples, constructing dose–response curves, obtaining the frequency of dicentric chromosomes from the blinded samples, and calculating the estimated

Data set		Estimate	Standard error	t-Statistic	*p*-value
Female	C	0.01	0.00	4.52	< 0.001
	α	0.03	0.01	4.14	< 0.001
	β	0.03	0.00	13.40	< 0.001
Male	C	0.01	0.00	4.30	< 0.001
	α	0.02	0.01	4.00	< 0.001
	β	0.03	0.00	14.48	< 0.001

Table 1. Calibration curve coefficients and standard errors for female and male data sets. C is the constant of the calibration curve equation, and α and β indicate the coefficients of D and D^2, respectively.

Group	Age (years)	Mean (years)	Standard deviation
A	20	20	
B	21, 26, 27, 28, and 35	27.4	5.00
C	23, 32, 34, and 58	36.8	15.00
D	29, 32, 33, 34, 38, 46, 51, and 67	41.3	12.80
E	20, 34, 39, 40, 51, 52, 52, and 54	42.8	11.80
F	43, 46, 47, and 50	46.5	2.90

Table 2. Ages of the donors used to establish the dose-response curves for each group.

Data set		Estimate	Standard error	t-Statistic	*p*-value
Pooled	C	0.01	< 0.001	6.13	< 0.001
	α	0.03	< 0.001	5.61	< 0.001
	β	0.03	< 0.001	19.47	< 0.001

Table 3. Calibration curve coefficients and standard errors for the pooled dose–response curve. C is the constant of the calibration curve equation, and α and β indicate the coefficients of D and D^2, respectively.

dose by applying it to the dose-response curves is necessary. However, using our automatic system to calculate the estimated dose for blinded samples without human intervention may not yield accurate results compared to conventional methods. Therefore, we introduced an RDNN to calculate the estimated dose[27].

We prepared samples for the 30 dose–response curves using blood donated by individuals of various ages and sexes. After setting the 30 dose–response curves as training data, we checked the corrected estimated doses for nine blinded samples using the RDNN. As shown in Fig. 3 and Supplementary Table S3, all samples were deemed "valid." These results indicate that to accurately calculate the estimated dose for blinded samples exposed to ≥ 2 Gy using an automatic system, constructing various dose–response curves is necessary. Additionally, using artificial neural networks based on this information to estimate the dose for blinded samples can yield more accurate results.

Estimating dose for blinded samples for ≤ 1 Gy

We used an automatic system to investigate blood from three healthy individuals (B4: 30-year-old female, B5: 39-year-old male, B6: 31-year-old male) exposed to five doses (0.2, 0.4, 0.6, 0.8, and 1 Gy) and checked whether the actual dose was within the 95% confidence interval of the estimated dose. We first calculated the estimated doses using a pooled dose–response curve from 30 individual samples according to the IAEA guidelines. Compared to the ≥ 2 Gy samples, all samples were deemed "valid" (Fig. 4a, Supplementary Table S4).

We also checked whether the type of dose–response curve affected the validity of the estimated doses for ≤ 1 Gy by calculating the estimated doses using group-specific and individual dose–response curves. We utilized the dose–response curve segmented into six groups to compute estimated doses for each sample. Of 108 datasets, 5 of the blinded samples were "invalid" (four in the 1 Gy sample and one in the 0.8 Gy sample) (Fig. 4b, Supplementary Table S5). In the 1 Gy samples, three were overestimated, and one was underestimated, with the difference between the lower or upper estimate values and the actual dose being significantly low, approximately ± 0.1 Gy.

When the estimated doses were calculated by applying them to 30 individual regression curves, approximately 92% of the data were valid (Fig. 4c). The lowest "valid" rate was obtained for the 0.2 Gy sample because the frequency of dicentric chromosomes was positioned lower than the intercept of each dose–response curve, resulting in no calculated upper or lower values. At 0.4 Gy, only two cases of invalid evaluations occurred, where the estimated doses were lower than the actual doses. Conversely, at the higher doses of 0.8 and 1 Gy, a tendency to be overestimated was observed. Specifically, five invalid evaluations occurred at 0.8 Gy—

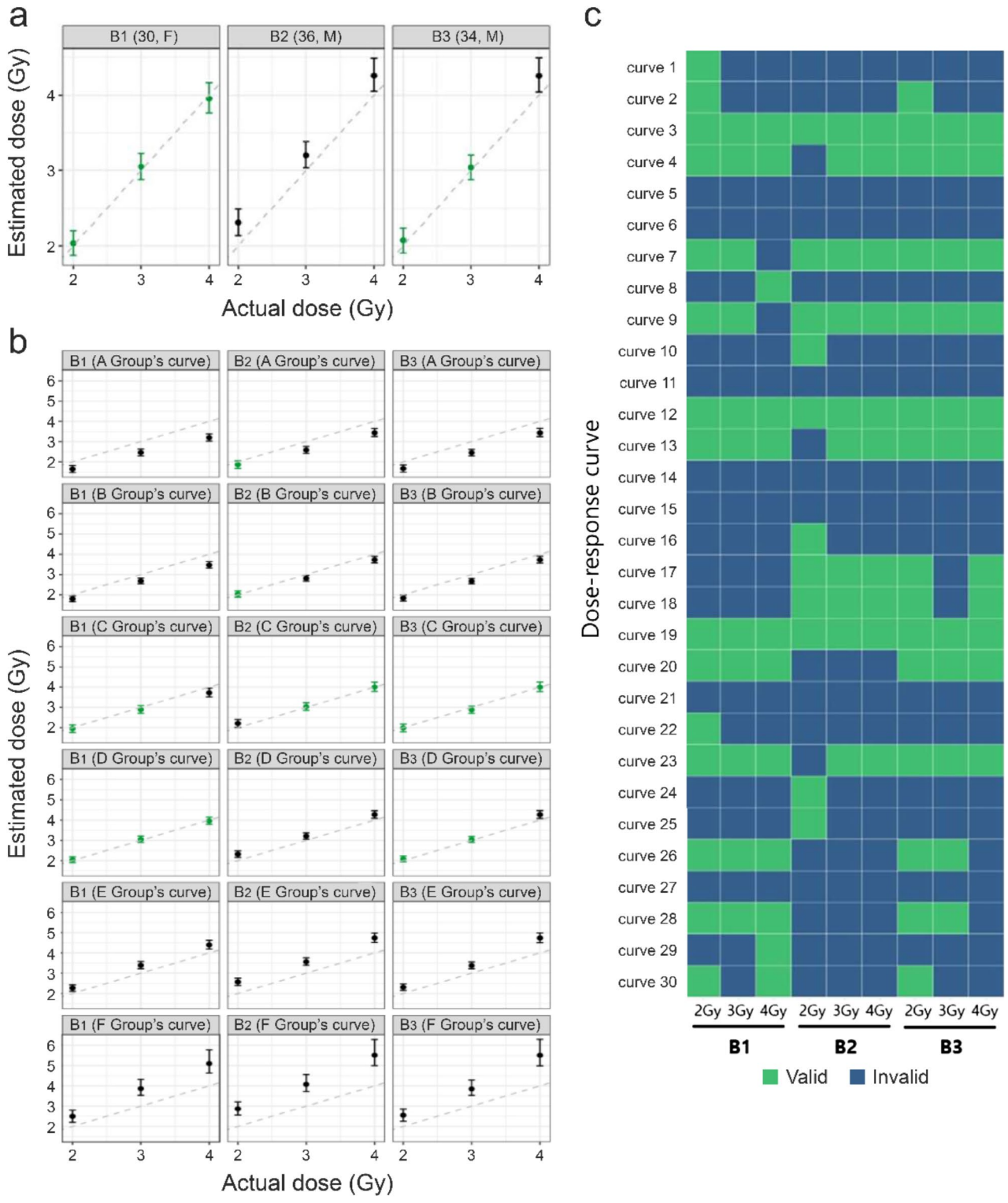

Fig. 2. Estimated absorbed doses for blinded samples irradiated at doses of ≥ 2 Gy. Error bars represent the 95% upper and lower confidence intervals. (**a**) Pooled dose–response curves are utilized to calculate the estimated doses. (**b**) Grouped dose–response curves are utilized to calculate the estimated doses. (**c**) Thirty dose–response curves are utilized to calculate the estimated doses. A sample is marked "valid" (green) if the actual dose is within the 95% confidence interval of the estimated dose; otherwise, it is considered "invalid" (black for **a**, **b**; blue for **c**).

Data set		Estimate	Standard Error	t-Statistic	*p*-value
Group A	C	0.01	< 0.001	2.54	0.13
	α	0.03	0.01	4.22	0.03
	β	0.04	< 0.001	15.77	< 0.001
Group B	C	0.01	< 0.001	6.27	< 0.001
	α	0.03	0.01	4.87	< 0.001
	β	0.04	< 0.001	22.71	< 0.001
Group C	C	0.01	< 0.001	4.61	< 0.001
	α	0.02	0.01	2.95	0.01
	β	0.03	< 0.001	15.27	< 0.001
Group D	C	0.01	< 0.001	6.54	< 0.001
	α	0.03	< 0.001	7.94	< 0.001
	β	0.03	< 0.001	26.12	< 0.001
Group E	C	0.01	< 0.001	8.88	< 0.001
	α	0.02	< 0.001	6.50	< 0.001
	β	0.02	< 0.001	22.04	< 0.001
Group F	C	0.01	< 0.001	4.01	< 0.001
	α	0.03	0.01	4.26	< 0.001
	β	0.02	< 0.001	7.01	< 0.001

Table 4. Calibration curve coefficients and standard errors for grouped dose–response curves. C is the constant of the calibration curve equation, and α and β indicate the coefficients of D and D^2, respectively.

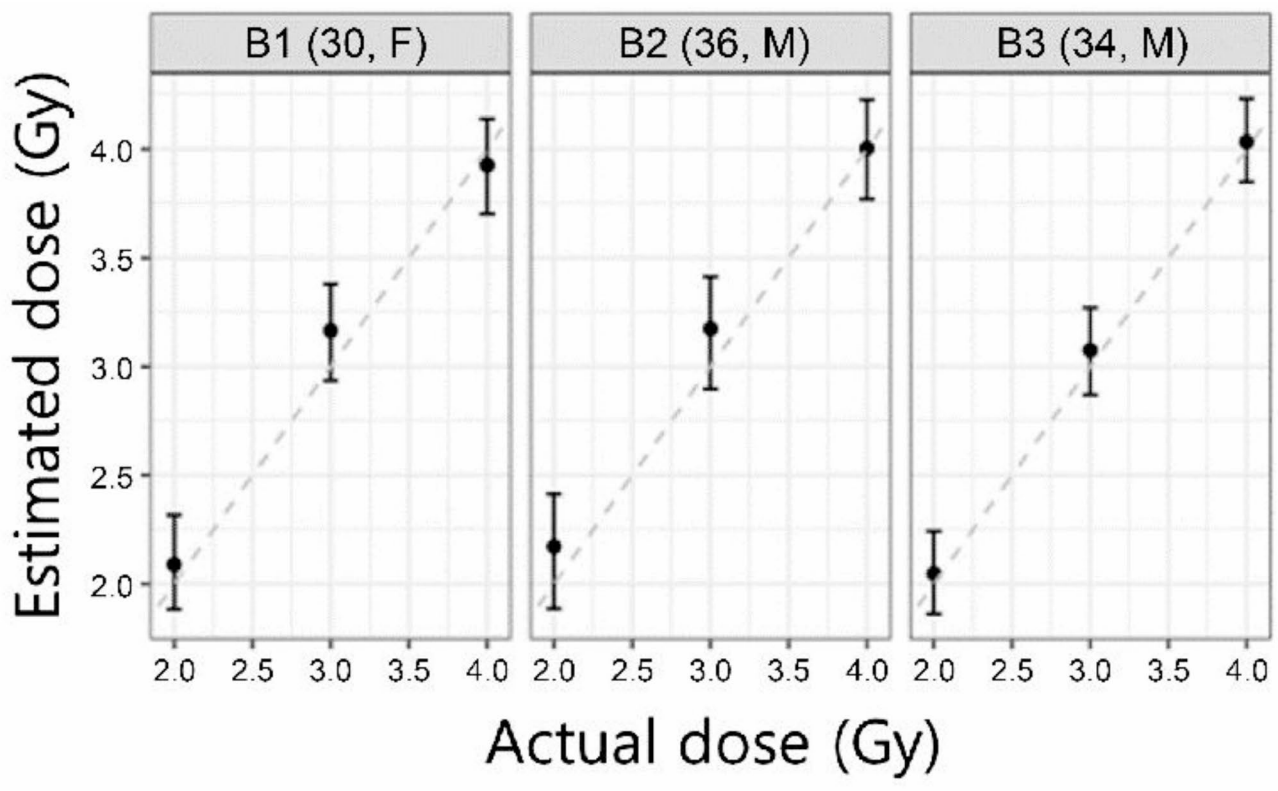

Fig. 3. Estimated absorbed doses for blinded samples irradiated at doses of ≥ 2 Gy. RDNN is utilized to calculate the estimated doses. Error bars represent the 95% upper and lower confidence intervals. RDNN, Regression Deep Neural Network.

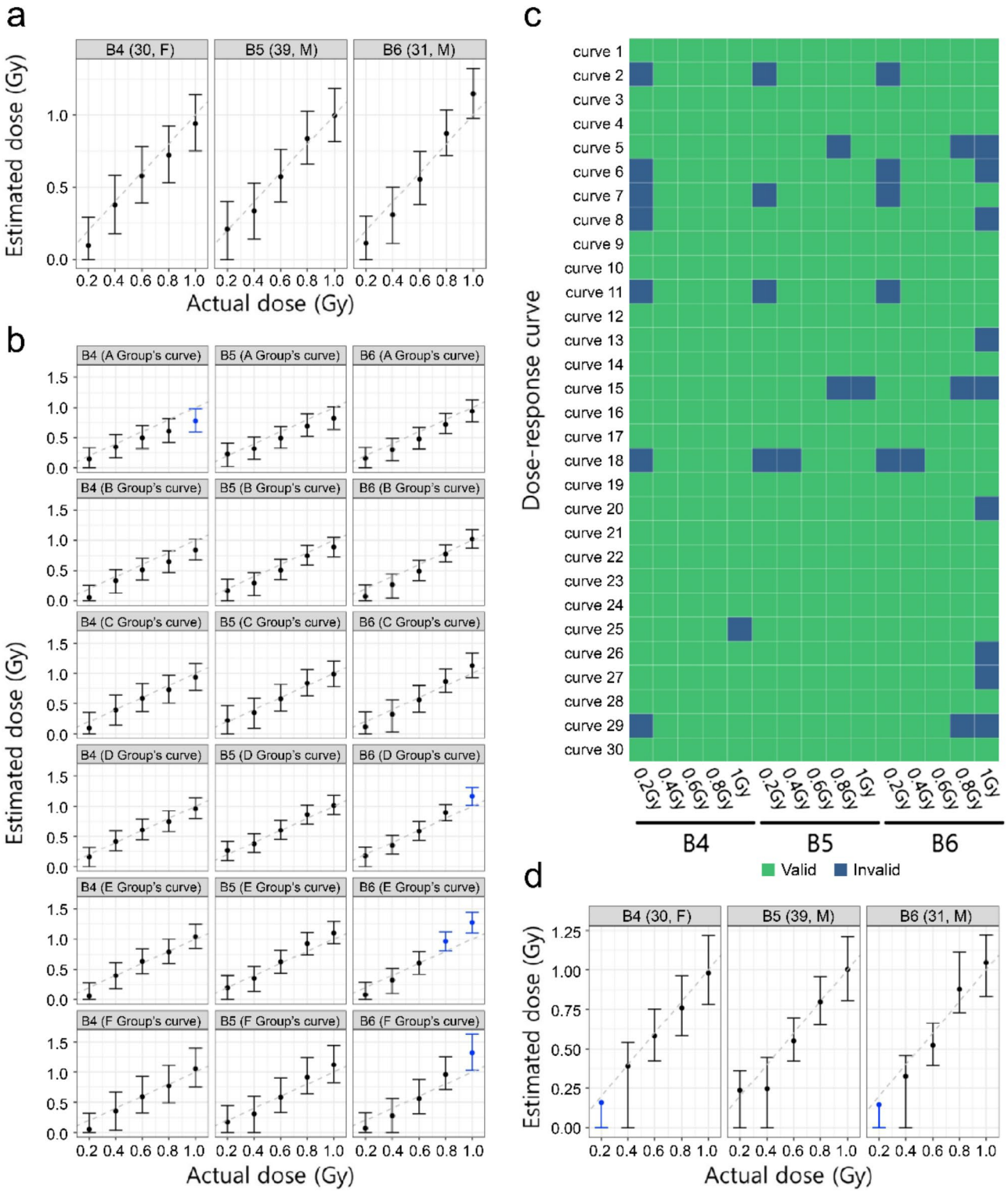

Fig. 4. Estimated absorbed doses for blinded samples irradiated at doses of ≤ 1 Gy. Error bars represent the 95% upper and lower confidence intervals. (**a**) Pooled dose–response curves are utilized to calculate the estimated doses. (**b**) Grouped dose–response curves are utilized to calculate the estimated doses. (**c**) Thirty dose–response curves are utilized to calculate the estimated doses. A sample is marked "valid" in black (**a**, **b**) or green (**c**) if the actual dose is within the 95% confidence interval of the estimated dose; otherwise, it is considered "invalid" (blue). (**d**) RDNN is used to calculate the estimated doses. RDNN, Regression Deep Neural Network.

all of which were overestimated. At 1 Gy, 11 cases were invalid, with 10 being overestimated and one being underestimated. The difference between the lower or upper estimate values and the actual dose for these cases was approximately ± 0.06 Gy on average.

These results indicate that the estimated dose for blinded samples ≤ 1 Gy was not significantly influenced by the type of dose–response curve. This may be because of the differences between individuals in identifying dicentric chromosomes using an automatic system with dose. As shown by the data from 30 dose–response curves, the frequency of dicentric chromosomal differences was lower in the 1 Gy treatment group (standard deviation = 0.01) than in the 4 Gy treatment group (standard deviation = 0.13).

We also verified whether the corrected estimated dose calculated using the RDNN provided accurate results for samples ≤ 1 Gy. As shown in Fig. 4d and 13 of the 15 samples underwent fitting evaluations for the corrected estimated dose. For B4 and B6 irradiated with 0.2 Gy, the 95% upper limit estimation was not calculated, leading to invalid evaluations. Nevertheless, the differences between the actual and estimated doses were 0.04 and 0.05, respectively, suggesting close alignment between them (Supplementary Table S6).

Based on these results, we can confirm that calculating the estimated doses not only for sample ≥ 2 Gy but also for those ≤ 1 Gy is possible using our automatic system. Moreover, when determining the estimated dose for sample ≤ 1 Gy using an automatic system, the choice of dose curve did not play a significant role compared to that in those ≥ 2 Gy.

Low dose assessment for occupational radiation exposure

To evaluate the feasibility of using an automatic system for the routine monitoring of occupational radiation exposure, we conducted a dose assessment on five radiation workers. All were male, with ages as follows: RW1–35, RW2–39, RW3–27, RW4–31, and RW5–34 years old. These workers were continuously monitored through Optically Stimulated Luminescence (OSL) badges worn during their work, which were replaced every 3 months to check for radiation exposure. Moreover, the detection limit for biological dosimetry using dicentric chromosomes is 0.1 Gy[32] Given that the radiation worker dose limits are 50 mSV per year or 100 mSV over 5 years[33], we sought to determine whether our automatic system could estimate doses as low as 0.1 Gy. Blood samples were collected two times to coincide with the OSL replacement schedule. To evaluate the system's accuracy, some blood samples taken during the second collection were intentionally exposed to 0.1 Gy for precise dosimetry assessment. Over the 3-month experimental period, OSL results for the five radiation workers indicated no exposure to radiation. We confirmed the sensitivity of our automatic system in detecting differences as low as 0.1 Gy and conducted comparisons using the Wilcoxon rank sum test between the first and second unirradiated blood samples (1st [0 Gy] and 2nd [0 Gy]) and between the second unirradiated blood samples (2nd [0 Gy]) and those irradiated at 0.1 Gy (2nd [0.1 Gy]). As shown in Fig. 5a; Table 5, the difference between the 2nd (0 Gy) and 2nd (0.1 Gy) samples was significant ($p < 0.05$) for all samples. Furthermore, when comparing the 1st (0 Gy) and 2nd (0 Gy) samples, we found no significant differences between the groups ($p > 0.05$), confirming the consistency of our measurements.

To verify whether the biological dosimetry results aligned with the OSL outcomes, we employed pooled dose-response curves from 30 individuals to estimate doses. Of samples expected to be 0 Gy, nine were confirmed to be 0 Gy, as shown in Fig. 5b and Supplementary Table S7. Only one sample was calculated; a very low dose of 0.01 Gy was determined for the second sample from RW3-2nd (0 Gy). Other samples exhibited dicentric chromosome frequencies below the minimum threshold (C = 0.01) established by the pooled dose–response curve. Consequently, these samples were also recorded as 0 Gy because further calculations were not possible. Subsequently, upon comparing these results from the RDNN for 0 Gy, the corrected estimated dose tended to be consistently higher than those obtained from the pooled dose–response curve. In the estimation process, while the RW2-2nd (0 Gy) and RW5-1st (0 Gy) initially had estimated doses of 0 Gy according to the pooled dose–response curve, the corrected doses determined using the RDNN approach were relatively higher at 0.06 Gy and 0.05 Gy, respectively. Conversely, RW3-2nd (0 Gy), which had the highest initial estimate among the 0 Gy samples according to the pooled dose–response curve, showed a comparatively lower corrected dose of 0.02 Gy in the RDNN dataset. This discrepancy is likely due to the different types of information utilized by the RDNN. Among the three samples, RW3-2nd (0 Gy) exhibited the highest dicentric chromosome frequency, resulting in the highest estimated dose when calculated using the pooled dose–response curve. However, the RDNN approach calculated higher corrected doses for RW2-2nd (0 Gy) and RW5-1st (0 Gy). This difference arises from their fragment frequencies, with RW2-2nd (0 Gy) at 0.130 and RW5-1st (0 Gy) at 0.181, both of which are higher than the 0.121 recorded for RW3-2nd (0 Gy). The influence of fragment frequency on the corrected dose calculations likely accounts for the discrepancies observed between the results from RDNN's corrected doses and those estimated using the pooled dose–response curve. We evaluated the capability of the automatic system to calculate alterations in the frequency of dicentric chromosomes in the samples exposed to 0.1 Gy. Except for RW5, the 95% lower estimation values were computed as 0 in all samples, which resulted in the actual doses being within the 95% confidence intervals of the estimated doses. In the case of 0.1 Gy, RDNN calculations did not yield upper or lower confidence intervals. However, the most substantial disparity between the actual and estimated doses was observed in the RW5 sample, with a difference of 0.15 Gy. These findings indicate that our automatic system can detect changes in dicentric chromosome frequency at 0.1 Gy, despite some observed variability. This suggests potential for routine occupational radiation monitoring, though further refinement is needed.

Discussion

This study was conducted to determine whether differences existed among individuals when dose–response curves were generated using an automatic system without human review. To investigate this, we constructed 30 dose–response curves by obtaining blood from 30 individuals.

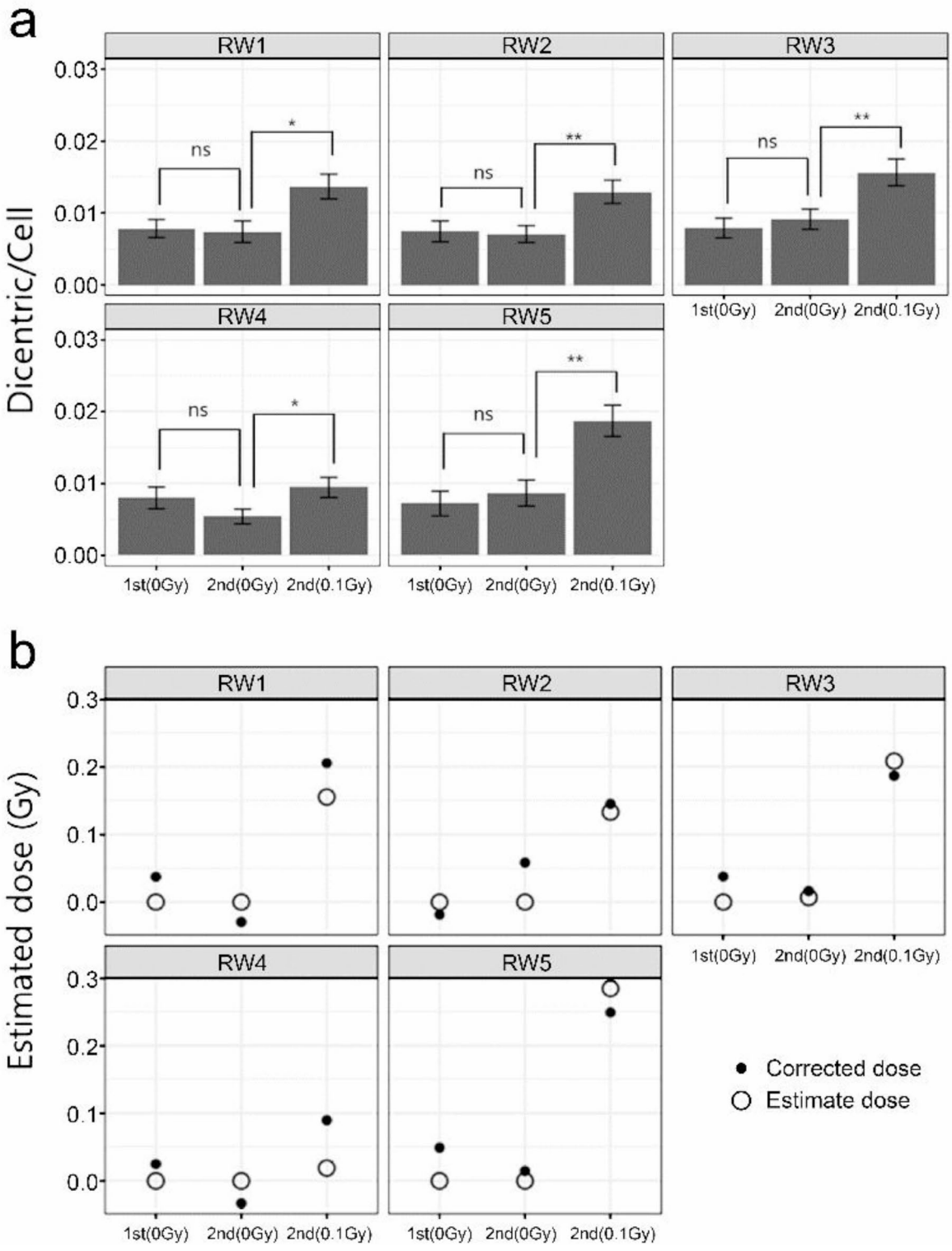

Fig. 5. Analysis of dicentric chromosome in five radiation workers using an automated system. (**a**) Comparison of the distribution of dicentric chromosome occurrences using an automatic system. The term "0 Gy" denotes samples that are not irradiated. (ns: $p > 0.05$, *: $p \leq 0.05$, **: $p \leq 0.01$, and ***: $p \leq 0.001$). (**b**) Estimated absorbed doses for radiation workers. Pooled dose–response curves and RDNN are utilized to calculate the estimated doses. The open circles represent the estimated doses obtained using pooled dose–response curves, while the closed circles represent the estimated doses obtained using RDNN. RDNN, regression deep neural network.

Sample			W-statistic	*p*-value
RW1	1st (0 Gy)	2nd (0 Gy)	7,880,691	0.82
	2nd (0.1 Gy)	2nd (0 Gy)	7,987,398	0.01
RW2	1st (0 Gy)	2nd (0 Gy)	8,645,575	0.84
	2nd (0.1 Gy)	2nd (0 Gy)	12,502,178	< 0.001
RW3	1st (0 Gy)	2nd (0 Gy)	11,080,577	0.71
	2nd (0.1 Gy)	2nd (0 Gy)	13,545,868	< 0.001
RW4	1st (0 Gy)	2nd (0 Gy)	8,720,780	0.14
	2nd (0.1 Gy)	2nd (0 Gy)	12,427,888	0.02
RW5	1st (0 Gy)	2nd (0 Gy)	3,286,997	0.55
	2nd (0.1 Gy)	2nd (0 Gy)	5,417,724	< 0.001

Table 5. Evaluation of differences in dicentric chromosome distribution between two groups. Comparison between the two samples is conducted using the Wilcoxon rank-sum test. The term "0 Gy" denotes samples that are not irradiated.

A critical aspect of this experiment was the preparation of the samples. All samples were prepared under identical conditions since the process of spreading and staining dicentric chromosomes can influence chromosome morphology. Since the accuracy of the automatic system changes with variations in chromosomal morphology has not been determined yet, we attempted to minimize the potential for incorrect scoring using the automatic system. Two researchers who created the training data for the automatic system prepared all of the 30 dose–response curves and blinded samples.

To determine differences among individuals, we established criteria based on age and sex and compared the differences accordingly. No significant differences were observed between the sexes; however, trends associated with age were evident. In particular, for the endpoint of the dose–response curve at 4 Gy, a higher frequency of dicentric chromosomes was found in donors aged between 20 years and early 30s. However, explaining the specific age-related characteristics beyond the late 30s has become challenging. Additionally, a survey on smoking, alcohol consumption, and medication use found no significant correlation with dicentric chromosomes in the background (0 Gy) group (Data not shown).

Since the purpose of constructing dose–response curves was to use them as reference data for blinded samples, a problem arose regarding whether a single dose–response curve could represent blood samples from various individuals exposed to radiation.

To resolve this issue, we categorized the samples into three groups (≥ 2, ≤ 1, and 0.1 Gy) and created blinded samples. The automatic system was used to determine whether suitable doses could be estimated for each part. We first investigated whether the pooled dose–response curves from the blood of three healthy donors exposed to 2, 3, and 4 Gy could be used to estimate the actual doses. Among the nine data points, five were within the 95% confidence interval of the actual doses, whereas the remaining four were overestimated.

In the subsequent analysis, we calculated estimated doses for the samples using both dose–response curves classified into six groups and 30 individual curves; however, we could not achieve satisfactory results.

To solve this problem, we used an artificial intelligence model. Following the approach suggested by Jang et al.[27], we trained an artificial neural network using dose–response curve datasets and then estimated the doses for the blinded samples. The results were promising; the actual doses for all nine samples were within a 95% confidence interval of the estimated doses. This finding indicates that when using an automatic system to calculate estimated doses ≥ 2 Gy without human intervention, employing an artificial neural network, such as an RDNN system, is more effective than conventional calculation methods, such as the root formula.

However, the process of estimating doses ≤ 1 Gy was different. Using conventional calculation methods[10], we found that all samples were covered by the pooled dose–response curve for 30 individuals, and 94.4% of the data points were satisfactory according to the group-specific dose–response curves. This finding suggested that choosing the dose–response curve for a particular individual is not critically important for estimating doses < 1 Gy. The standard deviation of the dicentric chromosome frequency among the 30 individuals exposed to 1 Gy was significantly lower than that among those exposed to 4 Gy. This notable discrepancy can be attributed to the lower mean values observed at 1 Gy, which were approximately 10.9% of those at 4 Gy. When calculating the relative dispersion using the coefficient of variation, the value was observed to be 17.8% for 1 Gy and 23.3% for 4 Gy. This shows that the difference is not substantial compared with the standard deviation values. Furthermore, this implies that the variation between individuals exposed to < 1 Gy was reduced owing to the inherently smaller mean values.

According to the ARS guidelines, for exposures < 1 Gy, monitoring the patient's condition rather than administering immediate treatment is recommended, along with considering the probabilistic effects that may arise in the future[6,31,34]. Therefore, providing more detailed exposure doses for patients exposed to ≤ 1 Gy could be highly beneficial for follow-up care. To explore the feasibility of using an automatic system for this purpose, we investigated blinded samples exposed to ≤ 1 Gy in 0.2 Gy intervals. The results showed that estimating the doses at these intervals for all samples was possible. However, since the blind samples in this study were primarily from individuals in their 30s, further validation across different age groups is needed to confirm the system's applicability to a broader population.

As the dose of the blinded sample decreased, the uncertainty increased, which was also evident in the third group of samples, where blood from radiation workers was used. We conducted a study with five radiation workers over 3 months to compare background levels and investigated the detectability of the smallest known dose unit that can be analyzed through dicentric chromosomes, which is 0.1 Gy.

Compared to the values obtained from the blinded sample tests at doses > 0.2 Gy, a greater discrepancy between the actual and estimated doses was found at lower doses. However, the estimated doses for all five blinded samples exposed to 0.1 Gy were within the 95% confidence interval, albeit with increased uncertainty compared with samples exposed to > 0.1 Gy (Supplementary Table S8). This indicates that although the results are sufficiently reliable for use, further studies are needed to derive more accurate values. Accordingly, developing methodologies to improve the accuracy at lower doses is needed. This could involve refining the automatic detection process, developing more sophisticated algorithms, or incorporating additional verification steps to accurately differentiate between true dicentric chromosomes and artifacts or anomalies detected by the system.

In conclusion, our findings confirm that the automatic system developed in this study enables accurate and rapid dose estimation for blinded samples ≥ 2 Gy and ≤ 1 Gy without human intervention. This study is the first to demonstrate the necessity of different approaches for estimating doses in samples exposed to < 1 Gy or > 1 Gy. Furthermore, the RDNN model developed here is applicable across all dose ranges for evaluating unknown samples, offering a unified approach to dose estimation. This highlights the potential of automated systems in radiation exposure assessments, contributing to improved accuracy and efficiency in dose estimation.

Materials and methods

Sample preparation

The study was conducted in accordance with the Declaration of Helsinki, and the protocol was approved by the Institutional Review Board of the Dongnam Institute of Radiological and Medical Sciences (DIRAMS) for all experimental procedures (approval no. D-1602-002-001). Prior to the collection of samples, informed consent was obtained from all participants under the supervision of the IRB of DIRAMS by signing a consent form containing the necessary details about the study. All methods were performed in accordance with relevant guidelines and regulations. To analyze dicentric chromosomes, blood samples were collected from healthy donors who were non-smokers at the time of the study and had no intentional radiation exposure for at least 3 months. Blood samples were irradiated with Cobalt-60 gamma rays (Gamma Beam X-200, Best Theratronics Ltd., Canada) at a dose rate of 0.3 Gy/min at 37 °C. To obtain reliable results, we constructed an in vitro irradiation setting that resembles an in vivo situation[35]. For the dose-response curves, blood samples were irradiated at 0.25, 0.5, 1, 2, 3, and 4 Gy and 2 h of incubation at 37 °C. Whole blood cells were cultured and fixed according to the IAEA's recommendation[10]. The fixed cells were spread on a microscope slide (Matsunami, Osaka, Japan) and stained with 5% Giemsa solution for 10 min. The automated Metafer4 system (MetaSystems Hard & Software GmbH, Altlussheim, Germany) was used for the auto-capture of metaphases at 63× magnification, and export of the jpg file and dicentric and monocentric chromosomes were identified using an automatic system.

Dose response curve fitting

The pooled dose-response curve was constructed using an application integrated into our automatic system[27], adhering to the calculation method proposed by H. Braselman[10]. To create the grouped and individual dose-response curves, we utilized the fitting function of the biodosetools package[28], with all analyses conducted in R version 4.2.2. The fitting formula is shown in Eq. (1)

$$Y = C + \alpha D + \beta D^2 \tag{1}$$

Does estimation

The blinded test sample was estimated using Merkle's approach[10]. Briefly, the upper and lower 95% confidence limits of the blind sample's estimated doses were calculated using the "calculate_aberr_table" and "estimate_whole_body_dose" functions of the biodosetools package. To calculate the estimated doses for blinded samples, we employed a RDNN algorithm, which is a component of our automatic system. In brief, we used chromosome count data identified by artificial intelligence from the dose-response curve as the input and the corresponding irradiated doses as the output. These data were used to train an RDNN, which accurately calculated the corrected doses for the blinded samples using these trained parameters.

Statistical analysis

The frequency data of the dicentric chromosomes used in the dose-response curve construction are provided in the supplementary data of Jang et al.[27], whereas the dicentric chromosome frequency data for blinded samples are presented in the Supplementary Table S9. Statistical analyses were performed using R version 4.2.2 (R Core Team). The correlation between age and dicentric chromosome frequency was analyzed using Pearson's correlation coefficient with the cor() function in R. To create a grouped dose-response curve, we performed a cluster analysis using only the 4 Gy results from 30 sets of dose-response data. Clustering was performed using hclust function of R. To compare dose responses by sex, we followed the method proposed by Paternoster et al.[29], with statistical significance determined at $p < 0.05$.

Data availability

All relevant data supporting the principal findings of this study are accessible within the article and its Supplementary Information files or can be from the corresponding author upon reasonable request.

Received: 5 July 2024; Accepted: 17 March 2025
Published online: 27 March 2025

References

1. Kudo, H. *Radiation Applications* (Springer, 2018).
2. Donya, M., Radford, M., ElGuindy, A., Firmin, D. & Yacoub, M. H. Radiation in medicine: Origins, risks and aspirations. *Glob Cardiol. Sci. Pract.* **2014**, 437–448 (2014).
3. Cucinotta, F. A., Kim, M. H. Y., Willingham, V. & George, K. A. Physical and biological organ dosimetry analysis for international space station astronauts. *Radiat. Res.* **170**, 127–138 (2008).
4. Garrett-Bakelman, F. E. et al. The NASA twins study: A multidimensional analysis of a year-long human spaceflight. *Science* **364**, 144 (2019).
5. Luxton, J. J. et al. Temporal telomere and DNA damage responses in the space radiation environment. *Cell. Rep.* **33**, 108435 (2020).
6. López, M. & Martín, M. Medical management of the acute radiation syndrome. *Rep. Pract. Oncol. Radiother.* **16**, 138–146 (2011).
7. Hafner, L., Walsh, L. & Schneider, U. Cancer incidence risks above and below 1 Gy for radiation protection in space. *Life Sci. Space Res. (Amst)* **28**, 41–56 (2021).
8. Cohen, B. L. Cancer risk from low-level radiation. *AJR Am. J. Roentgenol.* **179**, 1137–1143 (2002).
9. Furukawa, K. et al. Long-term trend of thyroid cancer risk among Japanese atomic-bomb survivors: 60 years after exposure. *Int. J. Cancer* **132**, 1222–1226 (2013).
10. Ainsbury, E. et al. Cytogenetic Dosimetry: Applications in Preparedness for and Response to Radiation Emergencies (IAEA, 2011).
11. ISO 21243. Radiation Protection- Performance Criteria for Laboratories Performing Initial Cytogenetic Dose Assessment of Mass Casualties in Radiological or Nuclear Emergencies-General Principles and Application to Dicentric Assay (ISO, 2008).
12. Port, M. et al. Rapid high-throughput diagnostic triage after a mass radiation exposure event using early gene expression changes. *Radiat. Res.* **192**, 208–218 (2019).
13. Romm, H. et al. The dicentric assay in triage mode as a reliable biodosimetric scoring strategy for population triage in large scale radiation accidents. *Proc. IRPA* 13 (2012).
14. Subramanian, U. et al. Automated dicentric aberration scoring for triage dose assessment: 60Co gamma ray dose-response at different dose rates. *Health Phys.* **119**, 52–58 (2020).
15. Lee, Y. H. et al. An intercomparison exercise to compare scoring criteria and develop image databank for biodosimetry in South Korea. *Int. J. Radiat. Biol.* **97**, 1199–1205 (2021).
16. Lee, Y. H. et al. Lessons on harmonization of scoring criteria for dicentric chromosome assay in South Korea. *Int. J. Radiat. Biol.* **100**, 709–714 (2024).
17. Abend, M. et al. Inter-laboratory comparison of gene expression biodosimetry for protracted radiation exposures as part of the RENEB and EURADOS WG10 2019 exercise. *Sci. Rep.* **11**, 9756 (2021).
18. Wilkins, R. C. et al. Interlaboratory comparison of the dicentric chromosome assay for radiation biodosimetry in mass casualty events. *Radiat. Res.* **169**, 551–560 (2008).
19. Jang, S. et al. Feasibility study on automatic interpretation of radiation dose using deep learning technique for dicentric chromosome assay. *Radiat. Res.* **195**, 163–172 (2021).
20. Shen, X. et al. High-precision automatic identification method for dicentric chromosome images using two-stage convolutional neural network. *Sci. Rep.* **13**, 2124 (2023).
21. Bayley, R. et al. Radiation dosimetry by automatic image analysis of dicentric chromosomes. *Mutat. Res.* **253**, 223–235 (1991).
22. Kim, K. et al. Deep neural network-based automatic dicentric chromosome detection using a model pretrained on common objects. *Diagnostics (Basel).* **13**, 3191 (2023).
23. Romm, H. et al. Automatic scoring of dicentric chromosomes as a tool in large scale radiation accidents. *Mutat. Res.* **756**, 174–183 (2013).
24. Lee, Y. et al. Application of a semi-automated dicentric scoring system in triage and monitoring occupational radiation exposure. *Front. Public. Health.* **10**, 1002501 (2022).
25. Alsbeih, G. A., Al-Hadyan, K. S., Al-Harbi, N. M., Judia, B., Moftah, B. A. & S. S. & Establishing a reference dose-response calibration curve for dicentric chromosome aberrations to assess accidental radiation exposure in Saudi Arabia. *Front. Public. Health.* **8**, 599194 (2020).
26. Jeong, S. K. et al. Dicentric chromosome assay using a deep learning-based automated system. *Sci. Rep.* **12**, 22097 (2022).
27. Jang, S. et al. Radiation dose estimation with multiple artificial neural networks in dicentric chromosome assay. *Int. J. Radiat. Biol.* **100**, 865–874 (2024).
28. Hernández, A. et al. Biodose tools: An R Shiny application for biological dosimetry. *Int. J. Radiat. Biol.* **99**, 1378–1390 (2023).
29. Paternoster, R., Brame, R., Mazerolle, P. & Piquero, A. Using the correct statistical test for the equality of regression coefficients. *Criminology* **36**, 859–866 (1998).
30. Cerezo, L. Radiation accidents and incidents. What do we know about the medical management of acute radiation syndrome? *Rep. Pract. Oncol. Radiother.* **16**, 119–122 (2011).
31. Donnelly, E. H. et al. Acute radiation syndrome: Assessment and management. *South. Med. J.* **103**, 541–546 (2010).
32. Gnanasekaran, T. S. Cytogenetic biological dosimetry assays: recent developments and updates. *Radiat. Oncol. J.* **39**, 159–166 (2021).
33. Korea Legislation Research Institute & Korea Law Translation Center. Enforcement decree of the nuclear safety act. https://elaw.klri.re.kr/kor_service/lawView.do?hseq=55843&lang=ENG
34. Ostheim, P. et al. Acute radiation syndrome-related gene expression in irradiated peripheral blood cell populations. *Int. J. Radiat. Biol.* **97**, 474–484 (2021).
35. Kye, Y. U. et al. Measurement of absorbed dose rate in water phantom maintained at body temperature by 60Co irradiator—comparison of experimental results and Monte Carlo simulation. *Nucl. Technol. Radiat. Prot.* **36**, 289–293 (2021).

Acknowledgements

This study was supported by a grant from the Korean Government (MSIT) to the Dongnam Institute of Radiological and Medical Sciences (DIRAMS; grant number 50491 – 2024).

Author contributions

Conceptualization, S.K.J. and S.J.O.; methodology, S.K.J., S.J.O., and M.H.J.; blood sample irradiation, Y.R.K., and H.J.K.; investigation, C.G.L., H.S.C., M.T.P., J.H.B., J.K.K, and J.S.K.; writing—original draft preparation, S.K.J., S.J.O., and M.H.J.; writing—review and editing, W.S.J.; supervision, S.K.J. and W.S.J.; project administration, S.K.J. and W.S.J. All authors have read and agreed to the published version of the manuscript.

Declarations

Competing interests
The authors declare no competing interests.

Additional information
Supplementary Information The online version contains supplementary material available at https://doi.org/10.1038/s41598-025-94678-8.

Correspondence and requests for materials should be addressed to S.K.J. or W.S.J.

Reprints and permissions information is available at www.nature.com/reprints.

Publisher's note Springer Nature remains neutral with regard to jurisdictional claims in published maps and institutional affiliations.